Linear Solvers for Collector Systems of Generalized Large-scale Inverter-Based Resources

Jongchan Choi
Grid Modeling and Controls Group
Oak Ridge National Laboratory
Knoxville, USA
choij1@ornl.gov

Suman Debnath
Grid Modeling and Controls Group
Oak Ridge National Laboratory
Knoxville, USA
debnaths@ornl.gov

***Abstract*—Collector systems for inverter-based resources (IBRs) are typically represented by equivalent circuits for electromagnetic transient (EMT) simulations. Recent studies have revealed that modeling a detailed collector system is essential to accurately represent the behavior of IBRs, especially when dealing with partial tripping during external disturbances. However, there are several challenges in simulating a detailed EMT model of a collector system due to the time required to simulate such systems. Thus, this paper investigates the modeling of a detailed collector system, taking into account its configuration and components as defined in IEEE standard 2800. The configurations include the collector systems of generalized large-scale IBR plants. The components include the main IBR transformer, collector bus, and feeders with lines and/or cables. The EMT model of the collector system is represented by differential algebraic equations (DAEs) that are discretized to form linear equations. Linear equations are solved using linear solvers. In this paper, linear solvers are proposed based on the Schur complement, which is utilized for simulation of the EMT model of collector systems of generalized large-scale IBRs to accelerate simulation speed while maintaining the accuracy of the results. The proposed solvers are verified by comparing the performance to that of linear solvers provided in MATLAB.**

***Index Terms*—Electromagnetic transient simulation, inverter-based resource, Schur complement, parallelism.**

I. Introduction

Inverter-based resources (IBRs), such as photovoltaic (PV) and wind power plants, are being increasingly deployed on the power grid [1]. Electromagnetic transient (EMT) models of IBRs are essential for ensuring the reliable operation of the power grid with increasing penetration of IBRs [2]. The reliability guidelines from the North American Electric Reliability Corporation (NERC) specify situations where EMT models are necessary, including IBR integration into weak grids, interactions between IBRs, control stability during disturbances, among others [2]. Additionally, multiple reports on disturbance analysis have highlighted the need for high-fidelity EMT models of IBRs to represent their behavior accurately when interacting with the power grid, especially in cases of partial tripping or momentary interruptions during external disturbances [3]–[6].

Collector systems for IBRs are typically represented using simplified impedance or equivalent circuits for EMT simulations in the past [7]–[9]. However, fully detailed collector systems representing each feeder and each line within IBRs are essential when developing a high-fidelity EMT model of IBRs. There has been some research to simulate an EMT model of the complete collector system that is discretized and thereafter, solved by using a matrix splitting method [10]. However, the matrix splitting method has limitations in terms of numerical instability that requires an additional capacitance when using this method. In addition, there are several challenges in simulating a detailed EMT model of a collector system due to the time required to simulate such systems. This is because large-scale IBRs have more complicated collector systems by having multiple collector buses within the collector system.

This paper investigates the modeling of the detailed collector system for generalized large-scale IBRs, taking into account its general configuration and components as defined in IEEE standard 2800. The components include the main IBR transformer, collector bus, and feeders with lines and/or cables. The EMT model of the collector system is represented by differential algebraic equations (DAEs) that are discretized to form linear equations. Linear equations are solved using linear solvers. In this paper, linear solvers are proposed based on the Schur complement [11], which is utilized for a double-bordered block diagonal matrix and a nested double-bordered block diagonal matrix to accelerate simulation speed while maintaining the accuracy of the results. The proposed solvers are verified by comparing the performance to that of linear solvers provided in MATLAB [12].

II. EMT Model of Collector System for Large-scale IBRs

The collector system of an IBR includes equipment and systems utilized to integrate IBR units within IBR as shown

Research sponsored by the Laboratory Directed Research and Development Program of Oak Ridge National Laboratory, managed by UT-Battelle, LLC, for the U. S. Department of Energy. This material is based upon work supported by ORNL DRD program INTERSECT initiative program number 32112883.

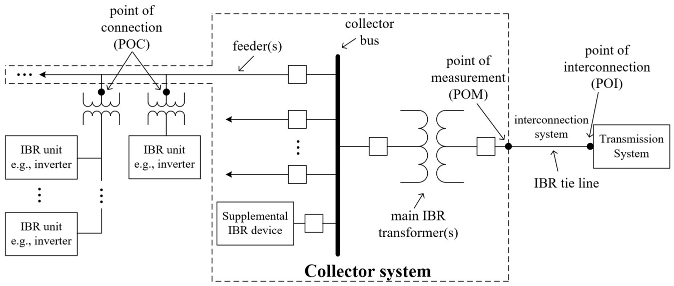

Fig. 1. Illustration of defined terms for ac-connected inverter-based resources (IBRs) [13]

in Fig. 1 [13]. This system includes multiple types of electrical components such as main IBR transformer(s), collector bus(es), feeder(s), and supplemental compensating devices between the point of connection (POC) of IBR units and the point of measurement (POM) of an IBR plant. An IBR unit is a cluster of multiple inverters connected together. A POC is the point where an IBR unit is interconnected with a collector system. The POC is the primary side of an IBR unit transformer (medium-voltage side) in this paper. A POM is the point between the primary side of a main IBR transformer (high-voltage side bus) and the interconnection system.

A. Main IBR Transformer

The main IBR transformer is a high-voltage power transformer that boosts up the collector system voltage (e.g., medium voltage) to the transmission system voltage (e.g., high voltage) at the POM as shown in Fig. 1. The number of main IBR transformers varies depending on the ratings of the IBR and the transformers. Main IBR transformers can be represented by the classical transformer model as shown in Fig. 2. The dynamics of the transformer can be expressed by the following DAEs (1)−(2).

$$(L_j^{P(s)} + L_m)\frac{di_{j,\text{grid}}^{P(s)}}{dt} + R_j^{P(s)} i_{j,\text{grid}}^{P(s)} - L_m \frac{di_{j,\text{grid}}^{s}}{dt} = -v_{j,\text{grid}}^{P(s)} \quad (1)$$

$$L_j^{P(s)} \frac{di_{j,\text{grid}}^{P(s)}}{dt} + R_j^{P(s)} i_{j,\text{grid}}^{P(s)} + L_j^{s} \frac{di_{j,\text{grid}}^{s}}{dt} + R_j^{s} i_{j,\text{grid}}^{s} = v_{j,\text{grid}}^{s} - v_{j,\text{grid}}^{P(s)} \quad (2)$$

where $v_{j,\text{grid}}^{p}$ are primary side voltages (j=a,b,c). $v_{j,\text{grid}}^{p}(s)$ are converted primary side voltages in the secondary side (j=a,b,c). $v_{j,\text{grid}}^{s}$ are secondary side voltages (j=a,b,c). n_s/n_p is turns ratio of the transformer. $L_j^{P(s)}$ and $R_j^{P(s)}$ are equivalent inductance and resistance of the primary side of the transformer converted in secondary side. L_j^{s} and R_j^{s} are equivalent inductance and resistance of the secondary side of the transformer. L_m is equivalent inductance for magnetizing currents of the transformer. $i_{j,\text{grid}}^{P(s)}$ are primary side currents converted into the secondary side (j=a,b,c). $i_{j,\text{grid}}^{s}$ are secondary side currents (j=a,b,c).

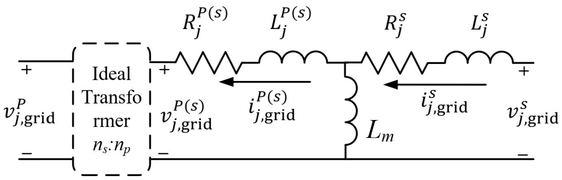

Fig. 2. Classical transformer model

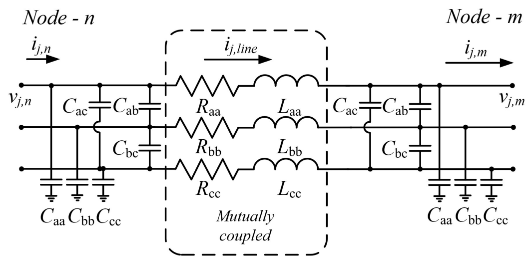

Fig. 3. Three phase PI section line model for feeders

B. Feeders

The feeders in IBRs are typically radial distribution lines by overhead lines or underground cables, which interconnect IBR units with the main IBR transformer of IBRs as shown in Fig. 1. Since multiple IBR units are collected by a feeder, there are many feeders within the collector system of large-scale IBRs. The feeders can be represented by a three-phase PI section line model due to its short lengths, accounting for mutual coupling effects among the three phases. The three-phase PI section model between nodes *n* and *m* for the feeders is illustrated in Fig. 3. The EMT model of the PI section line can be expressed by using the DAEs (3)−(5) provided below (phase a only):

$$L_{aa}\frac{di_{a,line}}{dt} + R_{aa} i_{a,line} + L_{ab}\frac{di_{b,line}}{dt} + R_{ab} i_{b,line} + L_{ca}\frac{di_{c,line}}{dt} + R_{ca} i_{c,line} = v_{a,n} - v_{a,m} \quad (3)$$

$$C_{aa}\frac{dv_{a,n}}{dt} + C_{ab}\frac{dv_{b,n}}{dt} + C_{ac}\frac{dv_{c,n}}{dt} = i_{a,n} - i_{a,line} \quad (4)$$

$$C_{aa}\frac{dv_{a,m}}{dt} + C_{ab}\frac{dv_{b,m}}{dt} + C_{ac}\frac{dv_{c,m}}{dt} = i_{a,line} - i_{a,m} \quad (5)$$

where, R_{ii}, L_{ii}, and C_{ii} (i=a,b,c) are self-resistance, self-inductance, self-capacitance of the PI section line model. R_{ij}, L_{ij}, and C_{ij} ($i \neq j$, i, j=a,b,c) are mutual-resistance, mutual-inductance, mutual-capacitance of the PI section line model.

C. Collector Bus and Collector System Configuration

The collector bus within the collector system is a conceptual bus that connects to the radial feeders as shown in Fig. 1. The collector bus generally connects multiple radial feeders in parallel with the main IBR transformers. Configuration of the collector system is determined by the connections of radial feeders and collector bus, generally a single collector bus with multiple radial feeders as shown in Fig. 4.

As the size of an IBR becomes larger, multiple collector buses can be presented within the collector system. Further

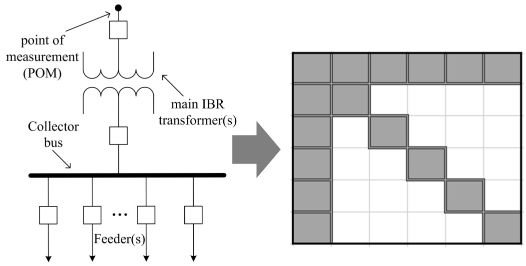

Fig. 4. Single collector bus with feeders (represented in a double-bordered block diagonal matrix)

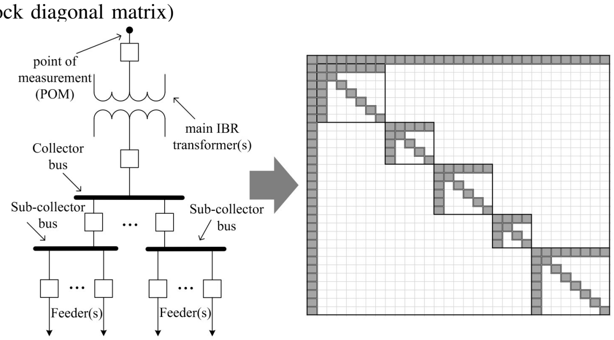

Fig. 5. Multiple collector buses with feeders (represented in a nested double-bordered block diagonal matrix)

more, multi-layered collector buses can be found for large-scale IBRs which are in actual practice installed in California. This also indicates multiple sub-collector buses can be collected by a super-collector bus to interconnect with the main IBR transformer. With multiple collector buses in large-scale IBRs, general configuration of the collector system can be illustrated as shown in Fig. 5.

For digital simulation, a system of linear equations for the collector systems can be formed by applying integration methods to the DAEs of the main IBR transformer and lines of the feeders as shown in Sections II-A and II-B. The system of linear equations can be presented in $\mathbf{Ax} = \mathbf{b}$. After appropriate matrix reordering, the A matrix of a collector system with a single collector bus can be expressed with a double-bordered block diagonal matrix as shown in Fig. 4. In case of a collector system with multiple collector buses, the A matrix can be expressed with a nested double-bordered block diagonal matrix as shown in Fig. 5. To effectively manage both double-bordered block diagonal matrices, linear solvers are proposed in the next section.

III. Linear Solvers for Double-bordered Block Diagonal Matrix

Linear solvers need to deal with a large A matrix while simulating the EMT model of collector systems in large-scale IBRs. The large A matrix needs to be operated on in every simulation time-step, which can be computationally extensive. Therefore, linear solvers based on the Schur complement and its nested technique are proposed to reduce the size of the operated matrix during simulations. With these proposed techniques, the simulation of collector systems can be accelerated while maintaining the accuracy of the simulation results.

A. Schur Complement Method for Single Collector Bus

The $\mathbf{A}$ matrix of collector system with double-bordered block diagonal matrix form can be expressed in (6)

$$\begin{bmatrix} \mathbf{A}_{11} & \mathbf{A}_{12} & \dots & \mathbf{A}_{1\mathrm{N}} \\ \mathbf{A}_{21} & \mathbf{A}_{22} & \mathbf{0} & \mathbf{0} \\ \vdots & \mathbf{0} & \ddots & \mathbf{0} \\ \mathbf{A}_{\mathrm{N}1} & \mathbf{0} & \mathbf{0} & \mathbf{A}_{\mathrm{NN}} \end{bmatrix} \begin{bmatrix} \mathbf{x}_1 \\ \mathbf{x}_2 \\ \vdots \\ \mathbf{x}_{\mathrm{N}} \end{bmatrix} = \begin{bmatrix} \mathbf{b}_1 \\ \mathbf{b}_2 \\ \vdots \\ \mathbf{b}_{\mathrm{N}} \end{bmatrix} \tag{6}$$

Eq. (6) can be expressed as

$$\mathbf{A}_{11}\mathbf{x}_1 + \mathbf{A}_{12}\mathbf{x}_2 + \dots + \mathbf{A}_{1\mathrm{N}}\mathbf{x}_{\mathrm{N}} = \mathbf{b}_1 \tag{7a}$$

$$\mathbf{A}_{21}\mathbf{x}_1 + \mathbf{A}_{22}\mathbf{x}_2 = \mathbf{b}_2 \tag{7b}$$

$$\vdots$$

$$\mathbf{A}_{\mathrm{N}1}\mathbf{x}_1 + \mathbf{A}_{\mathrm{NN}}\mathbf{x}_{\mathrm{N}} = \mathbf{b}_{\mathrm{N}} \tag{7c}$$

Eqs. (7b) and (7c) can be rearranged for $\mathbf{x_2}$ and $\mathbf{x_N}$ respectively as

$$\mathbf{x}_2 = \mathbf{A}_{22}^{-1}(\mathbf{b}_2 - \mathbf{A}_{21}\mathbf{x}_1) \tag{8a}$$

$$\vdots$$

$$\mathbf{x}_{\mathrm{N}} = \mathbf{A}_{\mathrm{NN}}^{-1}(\mathbf{b}_{\mathrm{N}} - \mathbf{A}_{\mathrm{N}1}\mathbf{x}_1) \tag{8b}$$

Substituting $\mathbf{x_2}$ and $\mathbf{x_N}$ in (7a) with (8a) and (8b) yields

$$\mathbf{A}_{11}\mathbf{x}_1 + \sum_{n=1}^{\mathrm{N}} \mathbf{A}_{1n}\mathbf{A}_{nn}^{-1}(\mathbf{b}_n - \mathbf{A}_{n1}\mathbf{x}_1) = \mathbf{b}_1 \tag{9}$$

Rearranging (9) results in

$$\mathbf{x}_1 = \left(\mathbf{A}_{11} - \sum_{n=1}^{\mathrm{N}} \mathbf{A}_{1n}\mathbf{A}_{nn}^{-1}\mathbf{A}_{n1}\right)^{-1} \times \left(\mathbf{b}_1 - \sum_{n=1}^{\mathrm{N}} \mathbf{A}_{1n}\mathbf{A}_{nn}^{-1}\mathbf{b}_n\right). \tag{10}$$

Once $\mathbf{x}_1$ is solved by (10), the rest of $\mathbf{x}_n$ $(n = 2, 3, ..., \mathrm{N})$ can be solved by (8a) through (8b). With this technique, the size of the operated A matrix is reduced from that of the complete A matrix to that of the block diagonal sub-matrices. Furthermore, it enables inherent parallelism when solving the rest of $\mathbf{x}_n$ $(n = 2, 3, ..., \mathrm{N})$ once $\mathbf{x}_1$ is known, they are independent of each other.

B. Nested Schur Complement Method for Multiple Sub-collector Bus

A collector system with multiple sub-collector buses presented in generalized large-scale IBRs can be represented by a nested double-bordered block diagonal matrix. To describe the nested Schur complement method, an outer double-bordered block diagonal matrix with two nested double-bordered block diagonal matrices are analyzed in this section. However, the number of nested double-bordered block diagonal matrices and the level of nested matrices may depend on the configuration of the collector system.

A nested double-bordered block diagonal matrix can be expressed in (11)

$$\begin{bmatrix} \mathbf{A}_{1,1} & \mathbf{A}_{1,2} & \mathbf{A}_{1,3} & \dots & \mathbf{A}_{1,\mathrm{k}} & \mathbf{A}_{1,\mathrm{k+1}} & \mathbf{A}_{1,\mathrm{k+2}} & \dots & \mathbf{A}_{1,\mathrm{N}} \\ \mathbf{A}_{2,1} & \mathbf{A}_{2,2} & \mathbf{A}_{2,3} & \dots & \mathbf{A}_{2,\mathrm{k}} & 0 & 0 & 0 & 0 \\ \mathbf{A}_{3,1} & \mathbf{A}_{3,2} & \mathbf{A}_{3,3} & 0 & 0 & 0 & 0 & 0 & 0 \\ \vdots & \vdots & 0 & \ddots & 0 & 0 & 0 & 0 & 0 \\ \mathbf{A}_{\mathrm{k},1} & \mathbf{A}_{\mathrm{k},2} & 0 & 0 & \mathbf{A}_{\mathrm{k},\mathrm{k}} & 0 & 0 & 0 & 0 \\ \mathbf{A}_{\mathrm{k+1},1} & 0 & 0 & 0 & 0 & \mathbf{A}_{\mathrm{k+1},\mathrm{k+1}} & \mathbf{A}_{\mathrm{k+1},\mathrm{k+2}} & \dots & \mathbf{A}_{\mathrm{k+1},\mathrm{N}} \\ \mathbf{A}_{\mathrm{k+2},1} & 0 & 0 & 0 & 0 & \mathbf{A}_{\mathrm{k+2},\mathrm{k+1}} & \mathbf{A}_{\mathrm{k+2},\mathrm{k+2}} & 0 & 0 \\ \vdots & 0 & 0 & 0 & 0 & \vdots & 0 & \ddots & 0 \\ \mathbf{A}_{\mathrm{N},1} & 0 & 0 & 0 & 0 & \mathbf{A}_{\mathrm{N},\mathrm{k+1}} & 0 & 0 & \mathbf{A}_{\mathrm{N},\mathrm{N}} \end{bmatrix} \begin{bmatrix} \mathbf{x}_1 \\ \mathbf{x}_2 \\ \mathbf{x}_3 \\ \vdots \\ \mathbf{x}_\mathrm{k} \\ \mathbf{x}_\mathrm{k+1} \\ \mathbf{x}_\mathrm{k+2} \\ \vdots \\ \mathbf{x}_\mathrm{N} \end{bmatrix} = \begin{bmatrix} \mathbf{b}_1 \\ \mathbf{b}_2 \\ \mathbf{b}_3 \\ \vdots \\ \mathbf{b}_\mathrm{k} \\ \mathbf{b}_\mathrm{k+1} \\ \mathbf{b}_\mathrm{k+2} \\ \vdots \\ \mathbf{b}_\mathrm{N} \end{bmatrix} \tag{11}$$

$$\mathbf{x}_1 = \left(\mathbf{A}_{1,1} - \sum_{n=3}^{\mathrm{k}} \mathbf{A}_{1,n}\mathbf{A}_{n,n}^{-1}\mathbf{A}_{n,1} - \mathbf{\Phi}(\mathbf{A}_{2,1} - \sum_{n=3}^{\mathrm{k}} \mathbf{A}_{2,n}\mathbf{A}_{n,n}^{-1}\mathbf{A}_{n,1}) - \sum_{n=\mathrm{k+2}}^{\mathrm{N}} \mathbf{A}_{1,n}\mathbf{A}_{n,n}^{-1}\mathbf{A}_{n,1} - \mathbf{\Omega}(\mathbf{A}_{\mathrm{k+1},1} - \sum_{n=\mathrm{k+2}}^{\mathrm{N}} \mathbf{A}_{\mathrm{k+1},n}\mathbf{A}_{n,n}^{-1}\mathbf{A}_{n,1})\right)$$

$$\times \left(\mathbf{b}_1 - \sum_{n=3}^{\mathrm{k}} \mathbf{A}_{1,n}\mathbf{A}_{n,n}^{-1}\mathbf{b}_n - \mathbf{\Phi}(\mathbf{b}_2 - \sum_{n=3}^{\mathrm{k}} \mathbf{A}_{2,n}\mathbf{A}_{n,n}^{-1}\mathbf{b}_n) - \sum_{n=\mathrm{k+2}}^{\mathrm{N}} \mathbf{A}_{1,n}\mathbf{A}_{n,n}^{-1}\mathbf{b}_\mathrm{n} - \mathbf{\Omega}(\mathbf{b}_\mathrm{k+1} - \sum_{n=\mathrm{k+2}}^{\mathrm{N}} \mathbf{A}_{\mathrm{k+1},n}\mathbf{A}_{n,n}^{-1}\mathbf{b}_n)\right) \tag{12}$$

$$where, \mathbf{\Phi} = (\mathbf{A}_{1,2} - \sum_{n=3}^{\mathrm{k}} \mathbf{A}_{1,n}\mathbf{A}_{n,n}^{-1}\mathbf{A}_{n,2})(\mathbf{A}_{2,2} - \sum_{n=3}^{\mathrm{k}} \mathbf{A}_{2,n}\mathbf{A}_{n,n}^{-1}\mathbf{A}_{n,2})^{-1}$$

$$\mathbf{\Omega} = (\mathbf{A}_{1,\mathrm{k+1}} - \sum_{n=k+2}^{\mathrm{N}} \mathbf{A}_{1,n}\mathbf{A}_{n,n}^{-1}\mathbf{A}_{n,\mathrm{k+1}})(\mathbf{A}_{\mathrm{k+1},\mathrm{k+1}} - \sum_{n=k+2}^{\mathrm{N}} \mathbf{A}_{\mathrm{k+1},n}\mathbf{A}_{n,n}^{-1}\mathbf{A}_{n,\mathrm{k+1}})^{-1}$$

Applying the Schur complement technique to the inner double-bordered block diagonal matrix in (11), solving it for $\mathbf{x}_2$ and $\mathbf{x}_{\mathrm{k+1}}$ yields

$$\mathbf{x}_2 = \left(\mathbf{A}_{2,2} - \sum_{n=3}^{\mathrm{k}} \mathbf{A}_{2,n}\mathbf{A}_{n,n}^{-1}\mathbf{A}_{n,2}\right)^{-1} \times \left(\mathbf{b}_2 - \sum_{n=3}^{\mathrm{k}} \mathbf{A}_{2,n}\mathbf{A}_{n,n}^{-1}\mathbf{b}_n\right) \tag{13a}$$

$$\vdots$$

$$\mathbf{x}_{\mathrm{k+1}} = \left(\mathbf{A}_{\mathrm{k+1},\mathrm{k+1}} - \sum_{n=\mathrm{k+2}}^{\mathrm{N}} \mathbf{A}_{\mathrm{k+1},n}\mathbf{A}_{n,n}^{-1}\mathbf{A}_{n,\mathrm{k+1}}\right)^{-1} \times \left(\mathbf{b}_{\mathrm{k+1}} - \sum_{n=\mathrm{k+2}}^{\mathrm{N}} \mathbf{A}_{\mathrm{k+1},n}\mathbf{A}_{n,n}^{-1}\mathbf{b}_n\right) \tag{13b}$$

Applying the Schur complement technique to the outer double-bordered block diagonal matrix in (11) by replacing $\mathbf{x}_2$ and $\mathbf{x}_{\mathrm{k+1}}$ from (13a) from (13b), then solving and rearranging it for $\mathbf{x}_1$ results in 12. Once $\mathbf{x}_1$ is solved by (12), the $\mathbf{x}_2$ and $\mathbf{x}_{\mathrm{k+1}}$ can be solved by (13a) and (13b). After the $\mathbf{x}_2$ and $\mathbf{x}_{\mathrm{k+1}}$ are solved, the rest unknowns from $\mathbf{x}_3$ to $\mathbf{x}_\mathrm{k}$ and $\mathbf{x}_{\mathrm{k+2}}$ to $\mathbf{x}_\mathrm{N}$ can be solved by the following expressions

$$\mathbf{x}_\mathrm{k} = \mathbf{A}_{\mathrm{k},\mathrm{k}}^{-1}(\mathbf{b}_\mathrm{k} - \mathbf{A}_{\mathrm{k},1}\mathbf{x}_1 - \mathbf{A}_{\mathrm{k},2}\mathbf{x}_2) \tag{14a}$$

$$\vdots$$

$$\mathbf{x}_n = \mathbf{A}_{n,n}^{-1}(\mathbf{b}_n - \mathbf{A}_{n,1}\mathbf{x}_1 - \mathbf{A}_{\mathrm{k},\mathrm{k+1}}\mathbf{x}_{\mathrm{k+1}}) \tag{14b}$$

The nested Schur complement technique enables inherent parallelism when solving $\mathbf{x}_2$ and $\mathbf{x}_{\mathrm{k+1}}$ as once $\mathbf{x}_1$ is known since they are independent of each other. In addition, this applies for solving the rest of $\mathbf{x}_n$ ($n = 2, 3, ..., \mathrm{k}$, and $\mathrm{k+2}, \mathrm{k+3}, ..., \mathrm{N}$) once $\mathbf{x}_2$ and $\mathbf{x}_{\mathrm{k+1}}$ are known.

IV. Simulation Results

In this section, simulation results are presented to evaluate the proposed techniques by comparing their effectiveness with that of commercial linear solvers provided in MATLAB, such as *linsolve()* and *mldivide()* [12]. To perform the simulations, the EMT model of two collector systems such as a single collector bus system and a multiple collector bus system, are discretized to form linear equations. Metrics of speed-up and maximum error are used to compare the effectiveness of the techniques. For speed-up measurements, the time measurements are calculated as an average execution time over 10,000 computations.

A. Single Collector Bus

The single collector bus system includes a main IBR transformer, a collector bus, and 5 radial feeders with different numbers of buses (i.e., 6, 8, 10, 12, and 14). In this case, the

TABLE I
COMPARISON OF LINEAR SOLVERS FOR SINGLE COLLECTOR BUS SYSTEM

	linsolve() from MATLAB	*mldivide()* from MATLAB	Schur complement (proposed)
Average Time [s]	9.268e-3	9.331e-3	0.470e-3
Maximum errors [%]	1.01e-12	1.01e-12	–
Speed-up	1x	0.99x	19.72x

system matrix is formed as a double-bordered block diagonal matrix upon discretization of the EMT model representing the collector system dynamics, which can be effectively managed by the Schur complement technique. The computation speed-up in solving the linear equation is compared with that of commercial linear solvers provided in MATLAB, as presented in Table I. In addition, the accuracy of the results is compared by calculating the maximum errors between the solvers, which are illustrated in Table I. As the results present, the Schur complement technique has achieved approximately a 19.7x speed-up while preserving accuracy.

B. Multiple Collector Buses

The multiple collector bus system includes a main IBR transformer, six collector buses (1 super-collector bus with 5 sub-collector buses), and 25 feeders. Unlike the single collector bus system, the super-collector bus connects to 5 sub-collector buses, and each sub-collector bus connects to 5 feeders (leveraged from the single collector bus system), resulting in a total of 25 feeders in the system. In this case, the proposed nested Schur complement technique to solve linear equations arising from the discretization of the EMT model of the collector system is more effective than the Schur complement technique due to the presence of nested double-bordered block diagonal matrices. The computation speed-up in solving the linear equations is compared between the Schur complement techniques and commercial linear solvers provided in MATLAB, which are presented in Table II. Additionally, the accuracy of the results is compared by calculating maximum errors between the solvers and illustrated in Table II. As can be seen from the results, the proposed nested Schur complement technique presents an approximately 48.2x speed-up over the commercial solvers while preserving accuracy, whereas an approximately 4.88x speed-up is observed from the Schur complement technique.

V. CONCLUSION

In this paper, EMT modeling of a detailed collector system is presented for generalized large-scale IBR plants. Models of main components, such as main IBR transformers, collector bus, and feeders are considered for the detailed collector system model. In addition, general configurations of the collector system are considered by including multiple sub-collector buses that can be found in actual large-scale IBRs installed in California. To effectively simulate EMT model of detailed collector systems of large-scale IBR, linear solvers based on the Schur complement are proposed to accelerate simulation. The detailed collector system and the proposed solvers were implemented in MATLAB to compare the solver's effectiveness with that of commercial solvers provided in MATLAB. The results presented that the proposed algorithms accelerate approximately up to 48.24 times faster while preserving accuracy.

TABLE II
COMPARISON OF LINEAR SOLVERS FOR MULTIPLE COLLECTOR BUS SYSTEM

	linsolve() from MATLAB	*mldivide()* from MATLAB	Schur complement (proposed)	Nested Schur complement (proposed)
Average Time [s]	40.103e-3	42.093e-3	8.217e-3	0.8314e-3
Maximum errors [%]	5.95e-10	5.95e-10	5.95e-10	–
Speed-up	1x	0.95x	4.88x	48.24x

REFERENCES

[1] NREL, "Examining Supply-Side Options to Achieve 100% Clean Electricity by 2035," National Renewable Energy Laboratory (NREL), Tech. Rep., 2022.

[2] NERC, "Reliability Guideline Electromagnetic Transient Modeling for BPS-Connected Inverter-Based Resources—Recommended Model Requirements and Verification Practices," North American Electric Reliability Corporation (NERC), Tech. Rep., 2023.

[3] NERC, "April and May 2018 Fault Induced Solar Photovoltaic Resource Interruption Disturbances Report," North American Electric Reliability Corporation (NERC), Tech. Rep., 2019.

[4] NERC, "San Fernando Disturbance," North American Electric Reliability Corporation (NERC), Tech. Rep., 2020.

[5] NERC, "Odessa Disturbance Texas Events: May 9, 2021 and June 26, 2021 Joint NERC and Texas RE Staff Report," North American Electric Reliability Corporation (NERC), Tech. Rep., 2021.

[6] NERC, "2023 Southwest Utah Disturbance Southwestern Utah: April 10, 2023 Joint NERC and WECC Staff Report," North American Electric Reliability Corporation (NERC), Tech. Rep., 2023.

[7] E. Muljadi, C. Butterfield, A. Ellis, J. Mechenbier, J. Hochheimer, R. Young, N. Miller, R. Delmerico, R. Zavadil, and J. Smith, "Equivalencing the Collector System of a Large Wind Power Plant," in *2006 IEEE Power Engineering Society General Meeting*, pp. 9 pp.–, 2006.

[8] M. U. Gul, A. Ahmed, and A. Warraich, "A Practical Method for Equivalencing of a Large Wind Farm with Multiple Turbine Representation," in *2018 IEEE 7th International Conference on Power and Energy (PECon)*, pp. 156–161, 2018.

[9] H. Meng, X. Ye, M. Yang, X. Song, Z. Su, W. Liu, L. Luo, and H. Zhao, "Equivalent Modeling and Simulation for PV System on Dynamic Clustering Equivalent Strategy," in *IECON 2017 - 43rd Annual Conference of the IEEE Industrial Electronics Society*, pp. 5779–5784, 2017.

[10] J. Choi and S. Debnath, "Electromagnetic Transient (EMT) Simulation Algorithm for Evaluation of Photovoltaic (PV) Generation Systems," in *2021 IEEE Kansas Power and Energy Conference (KPEC)*, pp. 1–6, 2021.

[11] Fuzhen Zhang, *The Schur Complement and Its Applications*, vol. 4. Springer, 2005.

[12] MATLAB. Systems of Linear Equations. [Online]. Available: https://www.mathworks.com/help/matlab/math/systems-of-linear-equations.html

[13] "IEEE Standard for Interconnection and Interoperability of Inverter-Based Resources (IBRs) Interconnecting with Associated Transmission Electric Power Systems," *IEEE Std 2800-2022*, pp. 1–180, 2022.